Chemical Physics Letters 549 (2012) 82–85

Contents lists available at SciVerse ScienceDirect

Chemical Physics Letters

journal homepage: www.elsevier.com/locate/cplett

Penetrated and aligned carbon nanotubes for counter electrodes of highly efficient dye-sensitized solar cells

Zhibin Yang, Li Li, Huijuan Lin, Yongfeng Luo, Ruixuan He, Longbin Qiu, Jing Ren, Huisheng Peng *

State Key Laboratory of Molecular Engineering of Polymers, Department of Macromolecular Science and Laboratory of Advanced Materials, Fudan University, Shanghai 200438, China

ARTICLE INFO

Article history:
Received 25 July 2012
In final form 28 August 2012
Available online 1 September 2012

ABSTRACT

Due to the unique structure and excellent properties, carbon nanotubes (CNTs) have been widely proposed as electrode materials. However, the CNTs typically appear in a format of networks in which charges have to hop through a lot of boundaries with low efficiency. Here we have described a pressing method to produce penetrated and aligned CNT films in which the generated charges can be rapidly separated and transported during the application as electrodes. As a demonstration, they were used as counter electrodes to fabricate dye-sensitized solar cell with an efficiency of ~8.46%, which was higher than the conventional platinum electrode.

1. Introduction

In the development of photovoltaic devices, it is critically important but remains challenging to discover new electrode materials to replace the conventional indium and platinum which have obvious disadvantages including high cost, complex fabrication, and chemical instability in corrosive electrolyte [1–6]. To this end, carbon nanotubes (CNTs) have recently attracted increasing attentions as a promising candidate because of their abundance, remarkable electrical conductivity [7,8], excellent electrocatalytic activity [9,10], and high stability [11–13]. Various approaches were explored to prepare CNTs films for electrode materials such as random dispersion [9], spray coating [14], gel coating [15], water-soluble treatment [16], and dry spinning [17]. In the resulting CNT films, however, CNTs are either horizontally aligned or interconnected to form networks [9,14–19]. Therefore, the generated charges have to hop through a lot of boundaries among CNTs before they can be transported through the CNT film with low efficiency, which greatly limits the photovoltaic performance. For instance, the energy conversion efficiencies of derived dye-sensitized solar cells by using the CNT film as counter electrode are relatively low [9–17]. Here we have described a pressing method to produce a penetrated and aligned CNT film in which charges can be rapidly separated and transported along the CNTs during the application for electrode. As a demonstration, the penetrated CNT film was used as counter electrode to fabricate dye-sensitized solar cell with energy conversion efficiency of ~8.46%, which was higher than the platinum (Pt) electrode under the same condition. This penetrated and aligned structure design may be also used to prepare other conductive one-dimensional nanosystems such as nanorod and nanotube besides CNT in the development of novel electrode materials [20].

2. Experimental section

CNT arrays were grown by chemical vapor deposition with Fe (1 nm)/Al_2O_3 (10 nm) on silicon substrate as catalyst typically at 750 °C. Ethylene was used as carbon source, and a mixture of Ar and H_2 was used as carrying gas. The flow rate of Ar, H_2, and C_2H_4 were typically 400, 25, and 75 sccm, respectively. A thickness of higher than 4 mm could be achieved for the CNT array. To prepare the aligned CNT film, the array was simply pressed from one side to another by a polytetrafluoroethylene roller with smooth surface. The resulting CNT film can be easily peeled off from the substrate. For the application as counter electrode in dye-sensitized solar cell, the CNT film was first transferred onto FTO glass (15 ohm/square) or flexible indium tin oxide on polyethylene naphthalate (15 ohm/square), followed by pressing through a heat-sealing machine with pressure of 0.3 MPa at room temperature. The CNT film was tightly attached on the conductive glass by van der Waals forces. The Pt was coated onto conductive glass by thermal decomposition of H_2PtCl_6 [21]. Here the film thickness of 10–40 μm had been mainly studied as it remained challenging to peel off integral thinner films from the substrate, while the thickness of the Surlyn frame between the working and counter electrodes was the same of 60 μm in the following dye-sensitized solar cells.

The working electrode was composed of a layer of nanocrystalline TiO_2 particles (diameter of 20 nm) with thickness of 14 μm and a light-scattering layer of TiO_2 particles (diameter of 200 nm) with thickness of 2 μm prepared by a screen printing technology. The working electrode was heated to 500 °C for 30 min and annealed in air. It was then immersed in aqueous 40 mM $TiCl_4$ at

* Corresponding author.
E-mail address: penghs@fudan.edu.cn (H. Peng).

0009-2614/$ - see front matter © 2012 Elsevier B.V. All rights reserved.
http://dx.doi.org/10.1016/j.cplett.2012.08.055

70 °C for 30 min and washed with de-ionized water and ethanol, followed by sintering at 500 °C for 30 min. After the temperature was decreased to 120 °C, it was immersed into 0.3 mM N719 solution in a mixture solvent of dehydrated acetonitrile and tert-butanol (volume ratio of 1/1) for ~16 h. The N719-incorporated electrode was carefully rinsed by dehydrated acetonitrile. The working and counter electrodes with a Surlyn frame of 60 μm as the spacer were sealed by pressing them together at a pressure of ~0.2 MPa and a temperature of 125 °C. The redox electrolyte (composed of 0.1 M lithium iodide, 0.05 M iodine, 0.6 M 1, 2-dimethyl-3-propylimidazolium iodide, and 0.5 M 4-tert butyl-pyridine in dehydrated acetonitrile) was introduced into the cell through the back hole of counter electrode. Finally, the hole was sealed with the Surlyn and a cover glass. In the case of a flexible cell, a TiO_2 mixture with 80% anatase and 20% rutile was added to ethanol with concentration of 20 wt.%. The suspension was coated onto the conductive substrate by a doctor blading method to produce the working electrode.

The thickness of CNT film was measured by Dektak 150 Step Profiler. The structure of CNT film was characterized by scanning electron microscopy (Hitachi FE-SEM S-4800 operated at 1 kV). Raman measurement was performed on Renishaw inVia Reflex with excitation wavelength of 514.5 nm and laser power of 20 mW. The electrical conductivity was obtained by a physical property measurement system (KEITHLEY 2182A nanocoltmeter with 6221A DC and AC current source). The resistivity change under bending was monitored by Agilent 34401A digital multimeter. The dye-sensitized solar cells were measured by recording J–V curves with a Keithley 2400 Source Meter under illumination (100 mW/cm^2) of simulated AM1.5 solar light coming from a solar simulator (Oriel-94023 equipped with a 450 W Xe lamp and an AM1.5 filter). The stray light was shielded by a mask with an aperture which was a little smaller than the working electrode. Cyclic voltammetry and electrochemical impedance spectroscopy were performed on CHI 660a electrochemical workstation.

3. Results and discussion

Figure 1a schematically shows the preparation of penetrated and aligned CNT film. A CNT array was first synthesized by a chemical vapor deposition process [22,23]. Figure S1 shows photograph of a typical CNT array. The CNT array was then pressed down along one direction by a roller. A typical scanning electron microscopy (SEM) image of CNT film by side view is provided in Figure 1b. The CNTs were penetrated from the bottom to the top in the film and highly aligned with an angle of ~1.4° relative to the substrate. The aligned structure of CNTs can be also observed from the top view of the film (Figure S2). The resulting CNT film can be easily peeled off from the silicon wafer or stabilized on conductive glass after the further pressing treatment. Figure S3 shows a typical CNT film on fluorine-doped tin oxide (FTO) with thickness of ~30 μm (Figure S3a). The CNT film exhibited a smooth surface with a small fluctuation on the level of tens of nanometers (Figure S3b). The CNT number density was calculated to be 10^{10}/cm^2 based on the average diameter of ~12 nm for CNTs (Figure S4). Here the CNT arrays with heights from 0.4 to 1.6 mm were mainly used, which produced CNT films with thicknesses from ~10 to ~40 μm.

Due to the penetrated structure of CNT film, the electrical conductivity in the normal direction was close to individual CNTs on level of 10^4 S/cm as electrons directly transport along CNTs through the film [24,25]. This high conductivity in the normal direction is critically important to improve the charge separation and transport for the electrode application [26–29]. Because of the closely aligned structure of CNTs, this film also showed high in-plane electrical conductivities on level of 10^2 S/cm. Here the parallel conductivity (along the rolling direction) was about 90% higher than the perpendicular conductivity (perpendicular to the rolling direction). The CNT film was flexible and stable. Both parallel and perpendicular conductivities remained almost unchanged when it was bent under different curvatures (Figures S5a and S5b). In addition, they were decreased by less than 1% and 2% after 500 bending cycles, respectively (Figures S5c and S5d).

For the application as counter electrode in dye-sensitized solar cell, it is also necessary to have a high electrocatalytic capability in the redox reaction of I^-/I_3^- pair. Here cyclic voltammetry was used to compare the catalytic property of CNT film with conventional platinum in an acetonitrile solution containing 10 mM LiI, 1 mM I_2, and 0.1 M $LiClO_4$ under the same condition [30]. Figure 2 shows two typical oxidation/reduction peaks for CNT films with different thicknesses. Peak-to-peak voltage separation (V_{PP}) is generally used to evaluate the catalytic activity of electrodes. The values of V_{PP} were decreased from 0.43 to 0.33 V with the increasing film thickness from 10 to 30 μm, and then stabilized at ~0.33 V with the further increase. An optimal thickness occurred at about 30 μm. In addition, it appeared that CNT films could more effectively catalyze the redox reaction of I^-/I_3^- couple than Pt electrode under certain conditions. The high catalytic activity was mainly due to a high surface area and open ends and aligned structure of CNTs. The high surface area provided large contact areas with electrolyte for catalysis, the open end provided more sensitive active sites compared with the closed end and sidewall [31,32], and the aligned structure favored charge transports and separations.

The CNT film which had been tightly attached on FTO glass by van der Waals forces was used as counter electrode to fabricate the dye-sensitized solar cell (Figure 3). Figure 4a compares J–V curves of the cells based on CNT films with different thicknesses

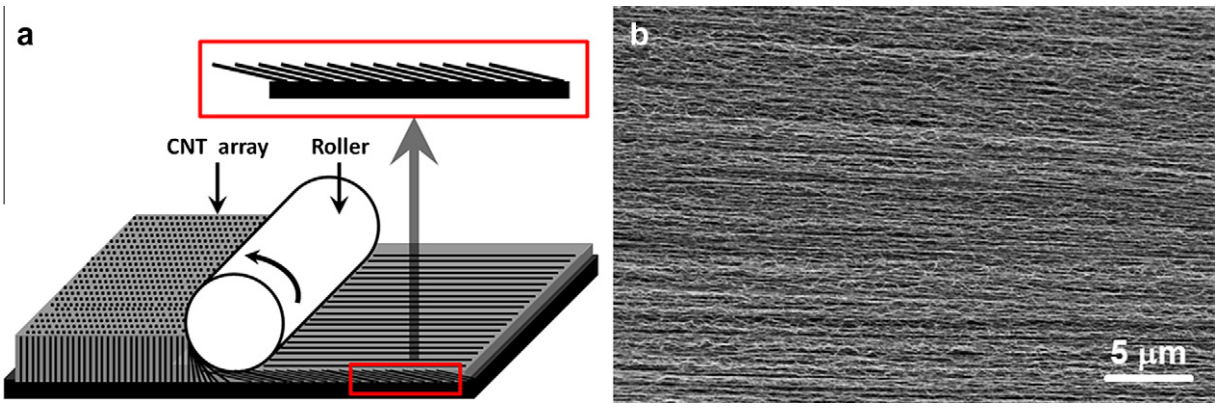

Figure 1. (a) Schematic illustration for the preparation of penetrated and aligned CNT film. (b) Scanning electron microscopy (SEM) image of the CNT film from a side view.

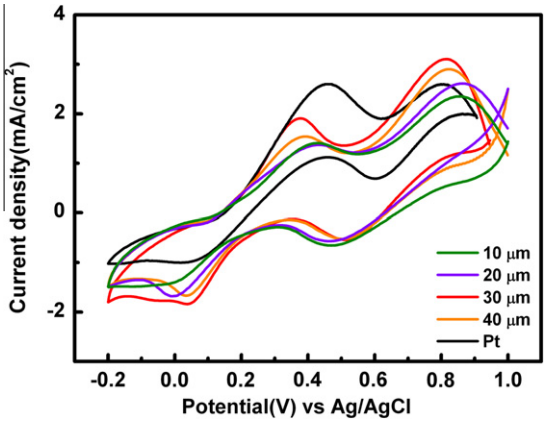

Figure 2. Electrocatalytic characterizations of penetrated and aligned CNT films with different thicknesses and platinum by cyclic voltammetry which was performed in an acetonitrile solution containing 10 mM LiI, 1 mM I_2, and 0.1 M $LiClO_4$ with a scan rate of 100 mV s^{-1} through a three-electrode setup.

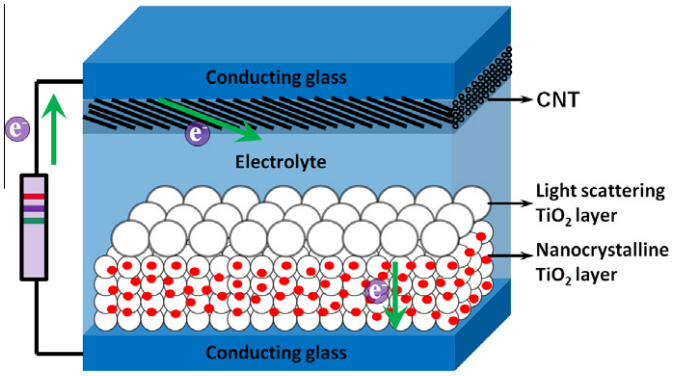

Figure 3. Schematic illustration of the dye-sensitized solar cell with penetrated and aligned CNT film as counter electrode.

from ~10 to ~40 μm, and the photovoltaic parameters are summarized in Table S1. The open-circuit photovoltage (V_{OC}) remained almost unchanged with the increasing thickness from ~10 to ~40 μm, while the fill factor (FF) increasing with the film thickness slightly increase from ~10 to ~20 μm and stabilized with the further increase of film thickness to ~40 μm. The short-circuit photocurrent density (J_{SC}) increased with the increasing thickness from ~10 to ~30 μm and then stabilized with the further increase of film thickness to ~40 μm. As a result, the energy conversion efficiency increased with the increasing film thickness from ~10 to ~30 μm and then stabilized with the further increase of film thickness. J_{SC} was increased with the increasing thickness from ~10 to ~30 μm as more CNTs increased contact areas with the electrolyte under the same CNT number density. For the CNT film with thickness of ~30 μm, the resulting cell typically showed V_{OC} of 0.726 V, J_{SC} of 17.35 mA/cm^2, and FF of 0.67, which produced an efficiency of 8.46%. As a comparison, the dye-sensitized solar cell based on the conventional Pt as counter electrode exhibited V_{OC} of 0.735 V, J_{SC} of 16.66 mA/cm^2, and FF of 0.60 (Figure 4a). The efficiency is calculated to be 7.32%. Therefore, such CNT films show promising applications as counter electrodes in dye-sensitized solar cells.

Electrochemical impedance spectroscopy was further used to understand the high performance of penetrated and aligned CNT film as counter electrode. Two semicircles are typically observed in the Nyquist plot (Figure 4b). The first semicircle represents the electrochemical reaction at counter electrode in the high-frequency region (i.e., R_{CT1}), while the second semicircle reflects the sum of the charge transfer at TiO_2/dye/electrode interfaces in the middle-frequency region (i.e. R_{CT2}) and the Warburg diffusion process of I^- and I_3^- ions in the electrolyte in the low-frequency region (i.e., R_{diff}) [14,33,34]. Obviously, the second semicircles derived from CNT films with different thicknesses are close in size, which indicates the same performance for both working electrode and electrolyte. Therefore, the catalytic activities among CNT films with different thicknesses can be mainly compared from the first semicircle. The dependence of the first semicircle size on thickness is similar to the cell efficiency.

Considering the requirements of practical applications, the cell performances had been also investigated under illuminations with different light intensities. Figure 5 compares J–V curves of the cells based on a penetrated and aligned CNT film with thickness of ~30 μm and Pt, and the detailed photovoltaic parameters are summarized in Table S2. The cell efficiencies are maintained to be relatively high for the different light intensities in both cases. However, the cell efficiencies based on the CNT film are always higher than those based on Pt as counter electrode under any light intensity. Here the similar power conversion efficiencies under different light intensities can be explained by the equation of $\eta = V_{oc}*J_{sc}*FF/P_{in}$. With the decreasing light intensity of P_{in}, both V_{oc} and FF were very close, but J_{sc} was decreased with almost the same amplitude as P_{in}, so the values of η were similar.

The cell stability also plays an important role in practical applications. Figure S6 shows the photovoltaic parameters with the time at room temperature. Both V_{OC} and J_{SC} were increased in the first five days and then slightly decreased, while FF was increased in the first ten days and then stabilized at 0.70. As a result, the

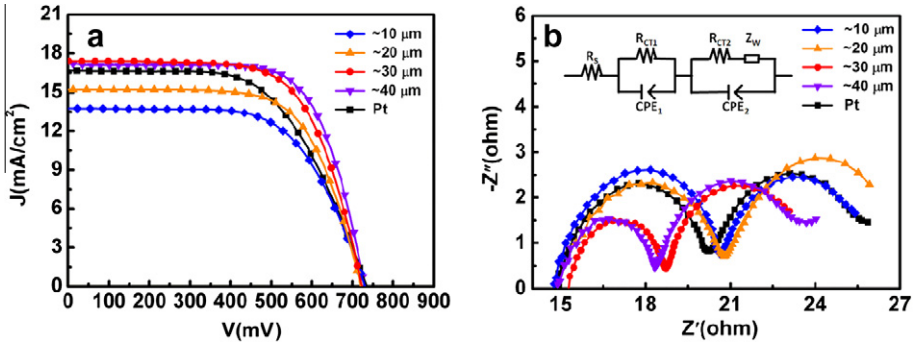

Figure 4. (a) J–V curves of dye-sensitized solar cells by using penetrated and aligned CNT films with different thicknesses and platinum (Pt) film as counter electrodes under AM1.5 illumination. (b) Nyquist plots of the cells at (a) (the inserted image showing an equivalent circuit). The frequencies were ranged from 0.1 to 100 kHz with an applied voltage of −0.8 V. Here R_S, R_{CT1}, R_{CT2}, Z_W, and CPE stand for serial resistance, charge-transfer resistance at the counter electrode, charge-transfer resistance at TiO_2/dye/electrode interfaces, diffusion impedance, and constant phase element, respectively.

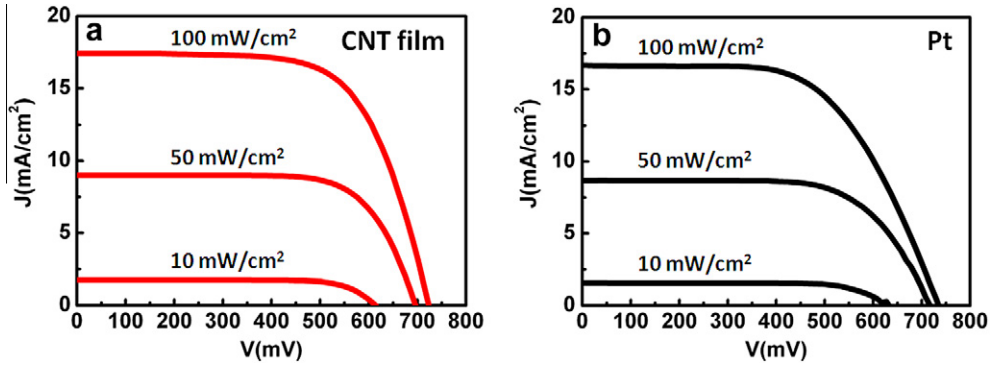

Figure 5. J–V curves of dye-sensitized solar cells based on a penetrated and aligned CNT film with thickness of ~30 μm (a) and Pt (b) as counter electrodes under AM1.5 illumination with different light intensities.

efficiency was increased from 8.41% to 8.85% in the first five days and then slightly decreased to 8.52% after one month.

The penetrated and aligned CNT films showed stable conductivities under bending, which enable promising application as flexible electrodes. Figure S7 shows a typical J–V curve of flexible dye-sensitized solar cell based on the CNT film with thickness of ~30 μm. The V_{OC}, J_{SC}, and FF are 0.748 V, 7.42 mA/cm^2, and 0.56, respectively, which produces an efficiency of 3.11%. Although it is currently lower than that of a rigid cell, it can be further increased by optimizing the used material, fabrication process, and cell structure.

It should be noted that CNT arrays can be also directly used as counter electrodes for dye-sensitized solar cells. Here the height of CNT arrays should be less than 40 μm. However, the growth of CNT arrays was very fast (typically 45–120 μm/min), and it was very difficult to obtain the required short CNT arrays. In addition, it was even more difficult to transfer these short CNT arrays with a large area from the silicon substrate without destroying them. Furthermore, CNT arrays generally could not maintain the original morphology after introduction of the liquid electrolyte during the fabrication of dye-sensitized solar cells [35]. Therefore, the use of CNT films was necessary to fabricate high-efficiency cells with high repeatability and high performance.

4. Conclusion

To summarize, penetrated and aligned CNT films with high electrical conductivity and high catalytic activity have been prepared as new counter electrodes to fabricate dye-sensitized solar cells. The resulting cells showed high energy conversion efficiencies up to 8.46%. In addition, flexible dye-sensitized solar cells had been easily made from these CNT films with high performance. The CNT films may be also widely used for other electrode materials in the case of being transparent, e.g., in replacement of indium tin oxide. Therefore, this penetrated and aligned conductive one-dimensional nanostructure can be developed to improve various photovoltaic and electronic devices.

Acknowledgements

This Letter was supported by NSFC (20904006, 91027025), MOST (2011CB932503, 2011DFA51330), MOE (NCET-09-0318), and STCSM (1052nm01600, 11520701400).

Appendix A. Supplementary data

Supplementary data associated with this article can be found, in the online version, at http://dx.doi.org/10.1016/j.cplett.2012.08.055.

References

[1] B. O'Regan, M. Grätzel, Nature 353 (1991) 737.
[2] A. Yella, H. Lee, H. Tsao, C. Yi, A. Chandiran, M. Nazeeruddin, E. Diau, C. Yeh, S. Zakeeruddin, M. Grätzel, Science 334 (2011) 629.
[3] Q. Zhang, G. Cao, Nano Today 6 (2011) 91.
[4] A. Hagfeldt, G. Boschloo, L. Sun, L. Kloo, H. Pettersson, Chem. Rev. 110 (2010) 6595.
[5] Y. Huang, E.M. Terentjev, ACS Nano 5 (2011) 2082.
[6] J.A. Rogers, T. Someya, Y.G. Huang, Science 327 (2010) 1603.
[7] (a) T. Chen, S. Wang, Z. Yang, Q. Feng, X. Sun, L. Li, Z. Wang, H. Peng, Angew. Chem. Int. Ed. 2011 (1815) 50;
(b) T. Chen, L. Qiu, Z. Cai, F. Gong, Z. Yang, Z. Wang, H. Peng, Nano Lett. 12 (2012) 2568.
[8] (a) H. Peng, M. Jain, D. Peterson, Y. Zhu, Q. Jia, Small 2008 (1964) 4;
(b) Z. Yang, X. Sun, X. Chen, Z. Yang, G. Xu, R. He, Z. An, Q. Li, H. Peng, J. Mater. Chem. 21 (2011) 13772;
(c) W. Guo, C. Liu, X. Sun, Z. Yang, H.G. Kia, H. Peng, J. Mater. Chem. 22 (2012) 903.
[9] W.J. Lee, E. Ramasamy, D.Y. Lee, J.S. Song, ACS Appl. Mater. Inter. 1 (2009) 1145.
[10] T. Chen, Z. Cai, Z. Yang, L. Li, X. Sun, T. Huang, A. Yu, H.G. Kia, H. Peng, Adv. Mater. 23 (2011) 4620.
[11] J.D. Roy-Mayhew, D.J. Bozym, C. Punckt, I.A. Aksay, ACS Nano 4 (2010) 6203.
[12] A. Hagfeldt, G. Boschloo, L.C. Sun, L. Kloo, H. Pettersson, Chem. Rev. 110 (2010) 6595.
[13] Y. Huang, E. M. Terentjev, ACS Nano 2011, 5, 2082.
[14] E. Ramasamy, W.J. Lee, D.Y. Lee, J.S. Song, Electrochem. Commun. 10 (2008) 1087.
[15] X. Mei, S. Cho, B. Fan, J. Ouyang, Nanotechnology 21 (2010) 395202.
[16] J. Han, H. Kim, D. Kim, S. Jo, S. Jang, ACS Nano 4 (2010) 3503.
[17] H. Peng, J. Am. Chem. Soc. 130 (2008) 42.
[18] P. Bradford, X. Wang, H. Zhao, J. Maria, Q. Jia, Y. Zhu, Compos. Sci. Technol. 2010 (1980) 70.
[19] D. Wang, P. Song, Ch. Liu, W. Wu, S. Fan, Nanotechnology 19 (2008) 075609.
[20] A. Ghicov, P. Schmuki, Chem. Commun. 20 (2009) 2791.
[21] N. Papageorgiou, W.E. Maier, M. Grätzel, J. Electrochem. Soc. 144 (1997) 876.
[22] M. Zhang, S.L. Fang, A.A. Zakhidov, S.B. Lee, A.E. Aliev, C.D. Williams, K.R. Atkinson, R.H. Baughman, Science 309 (2005) 1215.
[23] A.A. Kuznetsov, A.F. Fonseca, R.H. Baughman, A.A. Zakhidov, ACS Nano 5 (2011) 985.
[24] A. Bachtold, M. Henny, C. Terrier, C. Strunk, L. Forro, Appl. Phys. Lett. 73 (1998) 274.
[25] C. Berger, Y. Yi, Z.L. Wang, W.A. de Heer, Appl. Phys. A 74 (2002) 363.
[26] J. Wang, M. Musameh, Anal. Chem. 75 (2003) 2075.
[27] H. Zhu, H. Zeng, V. Subramanian, C. Masarapu, K. Huang, B. Wei, Nanotechnology 19 (2008) 465204.
[28] J.G. Nam, Y.J. Park, B.S. Kimc, J.S. Lee, Scr. Mater. 62 (2010) 148.
[29] J. Liu, Y. Kuo, K.J. Klabunde, C. Rochford, J. Wu, J. Li, ACS Appl. Mater. Interfaces 1 (2009) 1645.
[30] C.H. Yoon, R. Vittal, J. Lee, W.S. Chae, K.J. Kim, Electrochim. Acta 53 (2008) 2890.
[31] B.J. Landi, M.J. Ganter, C.D. Cress, R.A. DiLeo, R.P. Raffaelle, Energy Environ. Sci. 2 (2009) 638.
[32] S.W. Lee, Nat. Nanotechnol. 5 (2010) 531.
[33] A. Kay, M. Grätzel, Sol. Energy Mater. Sol. Cells 44 (1996) 99.
[34] K.M. Lee, C.W. Hu, H.W. Chen, K.C. Ho, Sol. Energy Mater. Sol. Cells 92 (2008) 1628.
[35] H. Peng, X. Sun, Chem. Commun. 45 (2009) 1058.